PERFORMANE EVALUATION OF THE FREE SPACE OPTICAL (FSO) COMMUNICATION WITH THE EFFECTS OF THE ATMOSPHERIC TURBULANCES

A Thesis

Submitted to the Department of Computer Science and Engineering

of

BRAC University

by

Md. Delower Hossen

Student ID: 05310044

Md. Golam Shaieen Alim

Student ID: 05310041

In Partial Fulfillment of the Requirements for the Degree

of

Bachelor of Science in Electronics And Communication Engineering

January 2008

BRAC University, Dhaka, Bangladesh

DECLARATION

I hereby declare that this thesis is based on the results found by myself. Materials of work found by other researcher are mentioned by reference. This thesis, neither in whole nor in part, has been previously submitted for any degree.

……..
(Dr. Satya Prasad Majumder)

Signature of Supervisor

…….....
(Md. Golam Shaieen Alim)

…….....
(Md. Delower Hossen)

Signature of Authors

ACKNOWLEDGMENTS

We want to express our sincere gratitude to our supervisor, Professor Satya Prasad Majumder, for his continuous guidance and support throughout our thesis at the BRAC University. His wisdom and kindness had been invaluable and made the whole thesis experience enjoyable

ABSTRACT

Free space optical (FSO) communication has emerged as a viable technology for broadband wireless applications which offers the potential of high bandwidth capacity over unlicensed optical wavelengths.Atmospheric turbulence has a significant impact on the quality of a laser beam propagating through the atmosphere over long distances. For optical wireless communication systems, most frequently used system is Intensity Modulated Direct Detection *(IM/DD)* system. For FSO systems, although the power efficiency is inferior to PPM, OOK encoding is more commonly used due to its efficient bandwidth usage and robustness to timing errors. In the presence of atmospheric turbulence, the received signal exhibits random intensity fluctuations which increase the BER. In this dissertation the characteristics and properties of several important design parameters are discussed with the modulation analysis and the link performance evaluated under considering the effects of the atmospheric turbulences which is the great challenges for the FSO.

TABLE OF CONTENTS

LIST OF TABLES

LIST OF FIGURES

Chapter 1

Introduction

1.1 Overview of Free Space Optical Communication

Optical wireless communication has emerged as a viable technology for next generation indoor and outdoor broadband wireless applications. Applications range from short-range wireless communication links providing network access to portable computers, to last-mile links bridging gaps between end users and existing fiber optic communications backbones, and even laser communications in outer-space links [1]. Indoor optical wireless communication is also called wireless infrared communication, while outdoor optical wireless communication is commonly known as free space optical (FSO) communication.

In applying wireless infrared communication, non-directed links, which do not require precise alignment between transmitter and receiver, are desirable. They can be categorized as either line-of-sight (LOS) or diffuse links. LOS links require an unobstructed path for reliable communication, whereas diffuse links rely on multiple optical paths from surface reflections. On the other hand, FSO communication usually involves directed LOS and point-to-point laser links from transmitter to receiver through the atmosphere. FSO communication over few kilometer distances has been demonstrated at multi-Gbps data rates [2].

FSO technology offers the potential of broadband communication capacity using unlicensed optical wavelengths. However, in-homogeneities in the temperature and pressure of the atmosphere lead to refractive index variations along the transmission path. These refractive index variations lead to spatial and temporal variations in optical intensity incident on a receiver, resulted in fading. In FSO communication, faded links caused by such atmospheric effects can cause performance degradation manifested by increased bit error rate (BER) and transmission delays [3].

FSO technology has also emerged as a key technology for the

development of rapidly deployable, secure, communication and surveillance systems, which can cooperate with other technologies to provide a robust, advanced sensor communication network. However, the LOS requirement for optical links reduces flexibility in forming FSO communication networks. Compared with broadcast radio frequency (RF) networks, FSO networks do not have an obvious simple ability to distribute data and control information within the network.

1.2 Comparison of Free Space Optical and Radio frequency technologies

Traditionally, wireless technology is almost always associated with radio transmission, although transmission by carriers other than RF waves, such as optical waves, might be more advantageous for certain applications. The principal advantage of FSO technology is very high bandwidth availability, which could provide broadband wireless extensions to Internet backbones providing service to end-users. This could enable the prospect of delay-free web browsing and data library access, electronic commerce, streaming audio and video, video-on-demand, video teleconferencing, real-time medical imaging transfer, enterprise networking and work-sharing capabilities [4], which could require as much as a 100 Mbps data rate on a sustained basis.

In addition, FSO permits the use of narrow divergence, directional laser beams, which if deployed appropriately, offer essentially very secure channels with low probability of interception or detection (LPI/LPD). Narrow FSO beams also have considerable obscuration penetrating capability. For example, penetration of dense fog over a kilometer distance is quite feasible at Gbps data rates with beam divergence of 0.1 mrad. The tight antenna patterns of FSO links allow considerable spatial re-use, and wireless networks using such connectivity are highly scalable, in marked contrast to ad-hoc RF networks, which are intrinsically non-scalable [5].

However, FSO has some drawbacks as well. Since a LOS path is required from transmitter to receiver, narrow beam point-to-point FSO links are subject to atmospheric turbulence and obscuration from clouds, fog, rain, and snow [2,6] causing performance degradation and possible loss of connectivity. In addition, FSO links can have a relatively short range, because the noise from ambient light is high, and also because the square-law nature of direct detection receiver doubles the effective path loss (in dB) when compared to a linear detector. Table 1.1 summarizes the difference between FSO and RF technologies.

Table 1.1: Properties of terrestrial FSO and RF communications.

	FSO Links	RF Links
Typical Data Rate	100 Mbps to ~Gbps	Less than 100 Mbps1
Channel Security	High	Low
Component Dimension	Small	Large
Networking Architecture	Scalable	Non-scalable
Source of Signal Degradation	Atmospheric turbulence and obscuration	Multipath fading, rain, and user interferences

Obviously, FSO communication will not replace RF communication, rather they will co-exist. Hybrid FSO/RF networks combine the advantages and avoid the disadvantages of FSO or RF alone. Even if the FSO connectivity cannot be provided all the time, the aggregate data rate in such networks is markedly greater than if RF links were used alone. RF alone does not have the band width for the transfer of certain types of data, for example high-definition video quality full-spectrum motion imagery. Hybrid wireless networks will provide maximum availability and capacity.

1.3 Free Space Optical Communication Systems

The major subsystems in an FSO communication system are illustrated in Fig. 1.1. A source producing data input is to be transmitted to a remote destination. This source has its output modulated onto an optical carrier; typically laser, which is then transmitted as an optic al field through the atmospheric channel. The important aspects of the optical transmitter system are size, power, and beam quality, which determine laser intensity and minimum divergence obtainable from the system. At the receiver, the field is optically collected and detected, generally in the presence of noise interference, signal distortion, and background radiation. On the receiver side, important features are the aperture size and the f/-number, which determine the amount of the collected light and the detector field-of-view (FOV).

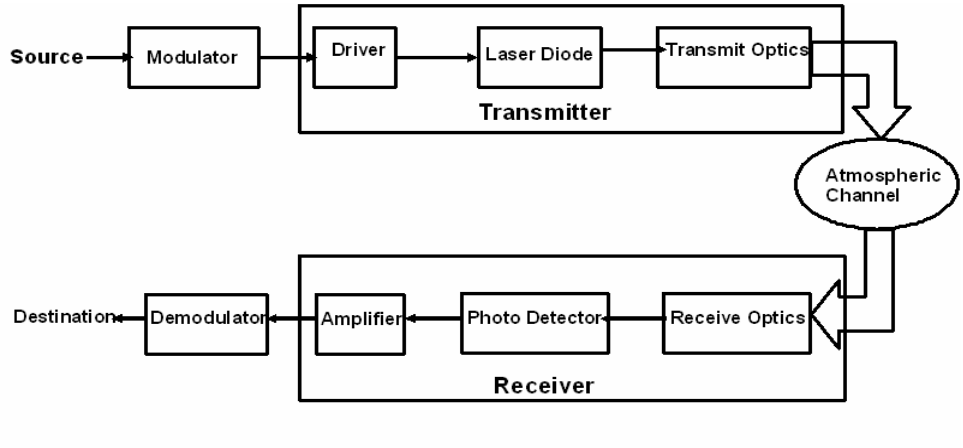

Figure 1.1: Block diagram of FSO communication system.

The modulation of the source data onto the electromagnetic wave carrier generally takes place in three different ways: amplitude modulation (AM), frequency modulation (FM), or phase modulation (PM), each of which can be theoretically implemented at any frequency. For an optical wave, another modulation scheme is also often used, namely intensity modulation (IM). Intensity is defined as flow energy per unit area per unit time expressed in W/m^2, and is proportional to the square of the field's amplitude. The light fields from laser

sources then pass beam forming optics to produce a collimated beam. This practice is equivalent to providing antenna gain in RF systems.

There are two basic types of optical receivers: non-coherent receivers and coherent receivers. Non-coherent receivers directly detect the instantaneous power of the collected optical field as it arrives at the receivers, thus are often called direct or power detection receivers. These receivers represent the simplest type of implementation and can be used whenever the transmitted information occurs in the power variation (i.e. IM) of the optical field. Coherent receivers, better known as heterodyne receivers, optically mix a locally generated light wave field with the received field, and the combined wave is photo detected. These receivers are used when information is modulated onto the optical carrier using AM, FM, or PM, and are essential for FM or PM detection.

The detection of optical fields is effected by various noise sources present at the receiver. The three dominant sources in FSO communications are: background ambient light, photo detector induced noise, and electronic thermal noise in circuits. Although background radiation may be reduced by the use of optical filtering, it still provides significant interference in the detection process. The detector quantum noise originates from the randomness of the photon counting process at the photo detector. The thermal noise can be modeled as additive white Gaussian noise (AWGN), whose spectral level is directly proportional to the receiver temperature.

1.4 Atmospheric Optical Channel

In FSO communication links, absorption of the beam by the atmosphere can be important, especially in adverse weather conditions of fog, snow, heavy rain, or obscuration. The combined effects of direct absorption and scattering of laser light can be described by a single path-dependent attenuation coefficient $\alpha(z)$

. The power received at receiver can easily be calculated for links without significant turbulence effects. The received power P_R for a receiver with receiver area ***A***, range ***L***, and beam divergence angle θ varies as [7]

$$P_R \approx \frac{A}{\pi\theta^2 L^2} e^{-\alpha L} P_T \tag{1.1}$$

Where $\mathbf{P_T}$ is the transmitted power, and α in this case is a constant value averaged over the propagation path ***L***.

The received power can be increased by increasing the transmitter power, the receiver area, or by reducing the beam divergence of the transmitter beam, which is diffraction limited. For FSO system with transmitted optical power of 10 mW, beam divergence of 1 mrad, and receiver diameter of 100 mm, the received power is still exponentially dependent on the atmospheric attenuation coefficient, as illustrated in Fig. 1.2. For a typical receiver sensitivity of -35 dBm, only an operational range less than 300 m can be achieved under heavy obscuration conditions. Even under light obscuration conditions, the link margin is reduced quite significantly compared with clear air conditions.

When turbulence effects are included, the effects of the atmosphere are in a sense more subtle. This optical turbulence is caused almost exclusively by temperature variations in the atmosphere, resulting in random variations of refractive index. An optical wave propagating through the atmospheric turbulence will experience random amplitude and phase fluctuations, which will generate a number of effects: break up of the beam into distinct patches of fluctuating illumination, wander of the centroid of the beam, and increase in the beam width over the expected diffraction limit. For longer links, the problems presented by atmospheric turbulence are quite severe [2, 3], since the average power received at the FSO receiver will decrease even more.

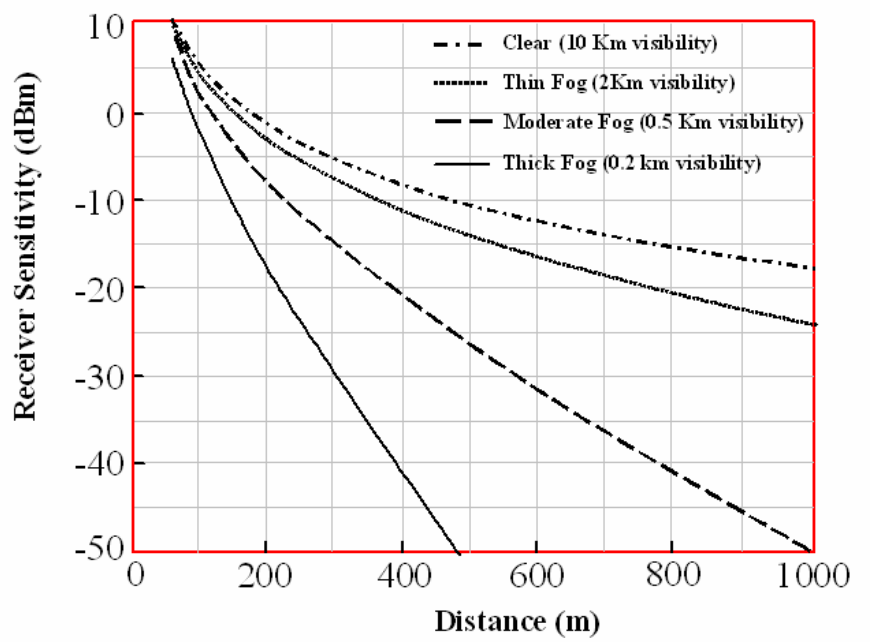

Figure 1.2: FSO link loss due to various atmospheric conditions (clear, thin fog, moderate fog, and thick fog), for system with P_T=10 mW, θ =1 mrad, and receiver diameter of 100 mm.

Besides power loss, the atmosphere may also distort the optical wave shape during propagation through dense clouds. This is particularly true for transmission of high power, narrow optical pulses, in which the atmospheric scattering can cause pulse broadening through multipath effects. Scattered pulse fields may be reflected toward the receiver and still have appreciable energy to produce a distorted optical pulse shape. If an optical pulse is transmitted from the source, the pulse signals along the scattered paths arrive with delays relative to the direct path and combine to yield a wider, broadened optical field pulse from that transmitted.

Chapter 2

Free Space Optical System Analysis And Design

2.1 Optical Sources and their Transmitted Fields

The key element in any optical communication system is an optical source that can easily be modulated. Such a source should produce energy concentrated in a narrow wavelength band, and should be capable of being modulated at very high rates. One of the primary sources of light in modern optical systems is the semiconductor laser. Their basic principles and characteristics, such as their output beam profile, will be important in assessing their performance when used in a free space optical (FSO) system.

2.1.1 Basic Characteristics of Semiconductor Lasers

A semiconductor laser consists of an active layer and surrounding *p*-type and *n*-type cladding regions, providing *p*-*n* junction geometry. The emission is realized in the active layer having an energy gap $\boldsymbol{E_g}$ that corresponds to the desired emission wavelength λ given by [8]

$$\lambda(\mu m) = \frac{1.240}{E_g(eV)} \tag{2.1}$$

The semiconductor material needed for emission should have a direct bandgap, meaning that the conduction band lies directly above the valence band in momentum space. Therefore, carriers can efficiently recombine to emit photons, since the momentum is conserved. hence the emitted wavelength is typically in the infrared spectrum.

When forward bias is applied to the active layer, carrier density is increased. As the pumping is increased further, a population inversion between conduction and valence bands will result. This is the condition where the electron density in the conduction band exceeds local electron density of the valence

band. In the population inversion condition, stimulated emission becomes greater than absorption, thus the active layer serves as an optical amplification medium, and the laser begins to oscillate. The feedback mechanism necessary for the laser oscillation is provided by two reflective facets at both ends of the active layer or laser cavity. In this process, there is noise component generated by the amplitude fluctuation of the signal light, called the relative intensity noise (RIN). Semiconductor lasers can produce high power levels, narrow linewidths (~1 nm), and low RIN(160 to 150 dB/Hz).

For optical communication applications single mode lasers are preferred, which contain only single longitudinal and transverse modes. To accommodate this requirement, laser configurations having a built-in frequency selective reflector are developed. Two common types of such lasers are: distributed feedback (DFB) lasers and distributed Bragg reflector (DBR) lasers [13, 14]. In DFB lasers, a Bragg grating formed along the cavity causes strong reflection at a certain wavelength, resulting in oscillation on a single mode with a narrower linewidth (< 0.1 nm). Therefore, no mode hoping occurs, so there is much less RIN. For the DBR lasers, the gratings are located at the ends of the active layer; hence no currents pass through the Bragg reflector regions. As a result, DBR lasers provide stable, tunable single mode operation while their other characteristics are similar to DFB lasers.

Table 2.1 summarizes basic characteristics of the semiconductor lasers [8].

Laser Materials	**III-V compounds**
Emission Wavelength	800 - 1500 nm
Output Power	1 - 100 mW
Linewidth	0.1 - 5 nm
Modulation Bandwidths	Up to many GHz

2.1.2 Wave Propagation in Free Space

The transverse modes of a laser system take the form of narrow beams of light that propagate between the mirrors of the laser resonator and maintain a field distribution that remains distributed around and near the axis of the system. While there are many solutions to this problem, it turns out that the simplest solution is called a Gaussian beam, which is appropriate to the laser under ordinary conditions. These beams have a characteristic radial intensity profile that expands laterally as they propagate. Gaussian beams are special solutions to the electromagnetic wave equation, which are restricted under paraxial conditions.

The free space propagation of a single mode laser beam can be modeled as the lowest order Gaussian beam wave, also called a TEM00 wave. Assuming the source is located at z=0, the field distribution of this fundamental mode at $z=L$ is given by [15]

$$U(r,L) = U_0 \frac{w_0}{w_L} \exp\left[- j(kL - \Phi) - r^2 \left(\frac{1}{w_L^{\,2}} + \frac{jk}{2R_L} \right) \right] \tag{2.2}$$

Where $\boldsymbol{r}$ is the transverse distance from the beam center, $\boldsymbol{w_0}$ is the minimum spot size, Φ is the phase shift, and $k = 2\pi/\lambda$ is the wave number. The beam parameters, $\boldsymbol{w_L}$ and R_L, are the spot size and the radius of curvature of phase front at L, respectively. They are defined as

$$w^2{}_L = w^2{}_0 \left[1 + \left(\frac{\lambda L}{\pi w^2{}_0} \right)^2 \right] \tag{2.3}$$

and

$$R_L = L \left[1 + \left(\frac{\pi w^2{}_0}{\lambda L} \right)^2 \right]$$

(2.4)

Thus, the form of the fundamental Gaussian beam is uniquely determined once the minimum spot size and its location are specified.

The spot size is the transverse distance at which the field amplitude is down by a factor $1/e$ compared to its value on the axis. The minimum spot size is the beam *spot* size at the plane ***z* =0**. From Eq. (2.3), it can be shown that w_L expands with distance ***L*** along the axis following a hyperbola that corresponds to the local direction of energy propagation. The angle between the asymptotes and the propagation axis is called beam divergence and is a measure of the angular beam spread. For an optical wave, the divergence is typically small and the half angle divergence θ_B can be written as [7]

$$\theta_B \approx \frac{\lambda}{\pi w_0} \tag{2.5}$$

The intensity of the optical wave is the squared magnitude of the field. Thus, the intensity distribution of the beam at **z=L** can be written as

$$I(r,L) = I_0 \frac{w^2{}_0}{w^2{}_L} \exp\left(-\frac{2r^2}{w_L{}^2}\right) \tag{2.6}$$

and Fig. 2.1 illustrates its expansion in free space propagation.

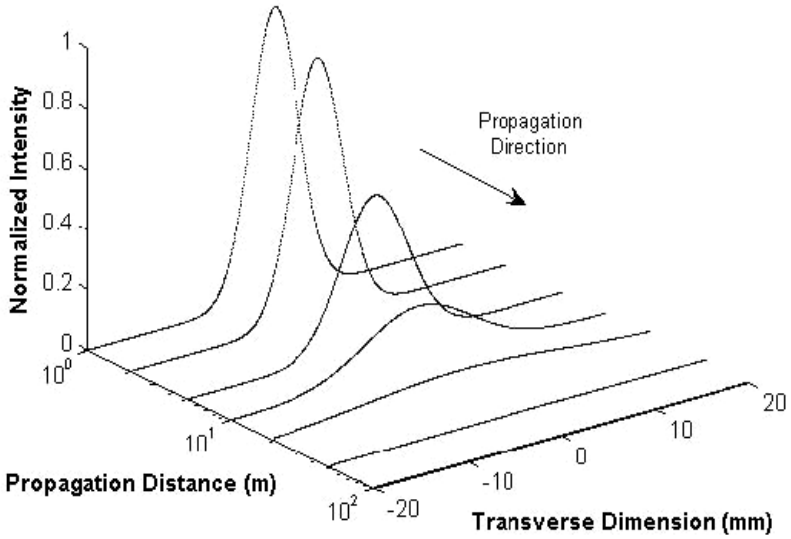

Figure 2.1: Intensity distribution profile in propagating Gaussian beam.

2.1.3 Beam Forming Optics

In long-range FSO communications, light fields from optical sources can be collected and refocused using beam forming optics, which will orient the light into particular directions. A combination of converging and diverging lenses placed at the source is used to produce a collimated beam. Fig. 2.2 shows a simple type of beam collimation commonly used in long- range links. For short-range links, in order to obtain omni directionality, the optical light needs to emerge over a wider angle, but at the expense of rapid beam expansion with distance.

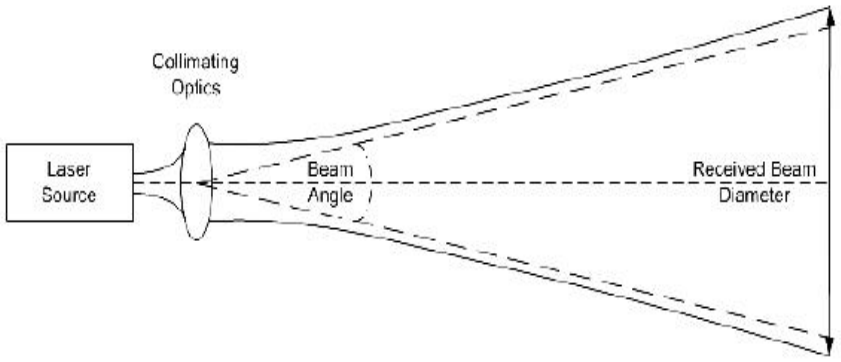

Figure 2.2: Example of beam collimation in long-range FSO links [7]

In an ideal collimation process, the converging lens focuses the light source to a point and the diverging lens expands it to a perfect beam. In practice, the source field is instead focused to a spot, and the expanded beam spreads during propagation with a planar beam diameter D_L of approximately

$$D_L = D_0\left[1+\left(\frac{2\theta_B L}{D_0}\right)^2\right]^{1/2} \qquad (2.7)$$

where D_0 is the output lens diameter, ***L*** is the distance from the lens, and θ_B is the transmitter beam angle, which for Gaussian beam is approximated by Eq. (2.5). At points in the near field, the emerging light is collimated with a diameter equals to the lens diameter, i.e. the light appears to uniformly exit over the entire lens. In the far field, the beam diameter expands with distance and appears as if the light is emerging from a single point. The expanding field far from the source is therefore confined to a two-dimensional solid angle Ω_B given by

$$\Omega_B = 2\pi\left[1-\cos(\theta_B)\right] \approx \pi\theta^2{}_B \qquad (2.8)$$

The advantage of beam forming can be emphasized by converting to an effective antenna gain parameter. From radio frequency (RF) theory, the effective antenna gain $\mathbf{G_A}$ can be written as

$$G_A = \frac{4\pi}{\Omega_B} \approx \frac{4}{\theta^2{}_B} \tag{2.9}$$

which is inversely proportional to the beam angle. For optical wavelengths, the beam angle is typically on the order of a few mrad, which corresponds to an antenna gain of 65 dB. This is a significant advantage compared to RF transmitters with typical beams on the order of degrees, which gives an antenna gain of about 40 dB.

2.2 Detection of Optical Radiation

When transmitted optical signals arrive at the receiver, they are converted to electronic signals by photo detectors. While there are many types of photo detectors in existence, photodiodes are used almost exclusively in optical communication applications because of their small size, suitable material, high sensitivity, and fast response time [17]. Two most commonly used photodiodes are the *pin* photodiode and the avalanche photodiode (APD) because they have good quantum efficiency and are made of semiconductors that are widely available commercially. For optimal design of the receiver system, it is important to understand the characteristics of these photodiodes and the noise associated with optical signal detection.

2.2.1 *pin* Photodiode

The *pin* photodiode consists of *p* and *n* regions separated by a very lightly *n*-doped intrinsic *i* region. In normal operation, a sufficient reverse bias voltage is applied across the device so that the intrinsic region is fully depleted. When an incident photon has energy greater than the band gap energy of the material, the photon can give up its energy and excite an electron from the valence band to the conduction band. This generates free electron-hole pairs called photo carriers. The *pin* photo detector is designed so that these photo carriers are

generated mainly in the depleted region, where most of the incident light is absorbed. The high electric-field present in the depletion region causes the photo carriers to separate and be collected across the reversed-bias junction. This produces a current flow in an external circuit, with one electron flowing for every photo carrier generated. The current flow is known as photocurrent.

The performance of a *pin* photodiode is often characterized by its responsivity $\Re$ given by [8]

$$\Re = \frac{\eta q}{h\nu} = \frac{i_S}{P_0} \tag{2.10}$$

where i_S is the average photocurrent generated by the optical power $\boldsymbol{P_o}$ incident on the photodiode. The quantum efficiency η is the number of the photo carriers generated per incident photon energy $h\nu$, and *q* is the electron charge. The parameter $\Re$ is quite useful since it specifies the photocurrent generated per unit optical power. The representative values for $\Re$ are 0.65 A/W for Si at 900 nm, 0.45 A/W for Ge at 1.3 μm, 0.9 A/W for InGaAs at 1.3 μm, and 1.0 A/W for InGaAs at 1.55 μm[17] .

2.2.2 Avalanche Photodiode

The APD internally multiplies the primary signal photocurrent before it enters the input circuitry of the following amplifier. This increases the receiver sensitivity, since the photocurrent is multiplied before encountering the thermal noise associated with the receiver circuit. In this structure, photocarriers are created initially mostly in the lightly *p*-doped intrinsic layer called a π -layer, because the n^+-*p* junction is very thin. When there is sufficient voltage across the π -layer, the photocarriers can drift rapidly across it. Therefore, at the n^+-*p*

junction near the positive electrode, a large field gradient is created and efficient avalanche multiplication occurs.

The performance of an APD is characterized by its multiplication factor *M* and is given by

$$M = \frac{i_M}{i_S} \qquad (2.11)$$

where i_M is the average value of total multiplied output current and i_S is the average un-multiplied photocurrent defined in Eq. (2.10). The avalanche mechanism is a statistical process, since not every photo carrier generated experiences the same multiplication. Thus, the measured value of *M* is expressed as an average quantity. It is also a function of the bias voltage. For practical applications, Si APD is operated typically with *M* =100. The reverse bias voltage ranges from 10 to 100 V. If the bias voltage is too high, the photodiode may be in danger of creating self-sustaining avalanche current without photo excitation, leading to extra noise from the photodiode [9]

Since an APD has much larger gain, it offers a better sensitivity than *pin* photodiode. The sensitivity increase may be on the order of 4 to 7 dB. However, they also have serious drawbacks, such as: a high operating voltage is required to provide a strong electric field, there is a strong temperature dependent of the multiplication factor, and there is additional noise due to saturation effects at high radiation levels [18]. Although these problems can be addressed and compensated, cost is increased. In contrast, a *pin* photodiode followed by an electronic amplifier could also provide good sensitivity margin with the expense of slower response time. For data transmission below one gigabit per second, the configuration of a *pin* photo detector and electronic amplifier may be advantageous over APD because of its low cost.

2.2.3 Noise in the Detection Process

The ability of a photo detector to detect an incoming signal is limited by intrinsic fluctuations or noise. If the signal power is less than the noise power, the signals will not be able to be distinguished clearly. The two most important sources of noise in the optical receiver are the shot noise resulting from the statistical nature of the photon-to-electron conversion process and the thermal noise associated with the amplifier circuitry. These sources of noise always accompany the optical signal. Another type of noise involved in the detection of optical radiation is dark current noise and background illumination noise, which may cause deleterious effects in FSO communication systems.

The principal noise associated with a photo detector is called quantum or shot noise. When an un odulated light wave is measured using a photo detector, two current components are obtained at the output. The first one is DC current, and the second one is the undesired shot noise signal. The shot noise arises from the statistical nature of the production and collection of discrete photoelectrons when an optical signal is incident on a photo detector. It has equal power density at all frequencies. If the electronic circuit after the photo detector only handles the frequency bandwidth Δf the mean-square current amplitude of the shot noise [9]

$$\left\langle i^2{}_{SN} \right\rangle = 2qi_S\Delta f \tag{2.12}$$

where ***q*** is the magnitude of electron charge and i_S is the average photocurrent as in Eq. (2.10).

For an APD, in addition to the primary source of shot noise, there is a noise figure associated with the excess noise generated by the random avalanche process. This noise figure $F(M)$ is defined as the ratio of the actual noise generated in an avalanche photodiode to the noise that would exists if all carrier pairs were multiplied by exactly *M* and is given by [9]

$$F(M) = \frac{\langle m^2 \rangle}{M^2} \tag{2.13}$$

where $\langle m^2 \rangle$ is the mean square gain and can be approximated as M^{2+x} with ***x*** varying between 0 and 1 depending on the material and structure. Thus, the mean- square current amplitude of the shot noise for APD [9]

$$\langle i_{SN}{}^2 \rangle_{APD} = 2qi_S M^2 F(M)\Delta f = 2qi_M MF(M)\Delta f \tag{2.14}$$

where i_S, i_M, and M are all defined as in Eq. (2.11).

Thermal noise, also called Johnson noise or Nyquist noise, is caused by the thermal agitation of charge carriers passing through a resistor. At temperatures above absolute zero, the thermal energy of the charge carriers in any resistor leads to fluctuations in local charge density. These fluctuating charges cause local voltage gradients that can derive a corresponding current into the rest of the circuit. If the circuits only handle a bandwidth of Δf and the resistance *R* is constant within this bandwidth, then the mean-square current amplitude of the Johnson noise $\langle i^2{}_{JN} \rangle$ is given by [9]

$$\langle i^2{}_{JN} \rangle = \frac{4kT\Delta f}{R} \tag{2.15}$$

R where ***k*** is the Boltzmann's constant and ***T*** is the absolute temperature. One way to reduce this noise is by cooling the offending component to a lower

temperature.

The dark current is the current that continues to flow through the bias circuit of the device even if no light is incident on the photodiode. It arises from electrons and/or holes that are thermally generated in the *p*-*n* junction of the photodiode. The dark current strongly depends on the type of semiconductor, operating temperature, and bias voltage; and is typically proportional to the term $\exp(-E_g / kT)$ *Depending* on the materials, their values range from 100 pA for Si up to 100 nA for Ge. Background illumination noise is caused by the light that is not part of the transmitted signals, such as ambient light. If the photodetector is not isolated from the background radiation, the appearance of this noise is inevitable. Due to the discreteness and randomness of both the dark current and background radiation, these noise sources are similar to the shot noise.

2.3 Link Physics of the Atmospheric Channels

The three primary atmospheric processes that affect optical wave propagation in free space are absorption, scattering, and refractive index fluctuations, or optical turbulence. Absorption and scattering by the constituent gases and particulates of the atmosphere give rise primarily to attenuation of the laser beam. Optical turbulence leads to receiver intensity fluctuations, beam broadening, beam wander, and beam break up; among other effects. Clearly, these deleterious effects have serious consequences in FSO communications.

2.3.1 Molecular Absorption and Scattering

Electromagnetic wave radiation is attenuated when propagating through the atmosphere due to absorption and scattering. Absorption occurs when a photon of radiation is absorbed by a gaseous molecule of the atmosphere, which converts the photon into kinetic energy or re-radiates it. Thus, absorption is a mechanism by which the atmosphere is heated. Atmospheric absorption is a

strong function of wavelength, where the most severe absorption occurs at ultraviolet wavelengths (below 200 nm) due to O_2 and O_3 molecules, while there is very little absorption at visible wavelengths (400 to 700 nm).

Similar to absorption, light scattering is also strongly wavelength dependent. Particles that are small in comparison with the wavelength (i.e. air molecules, haze) will produce Rayleigh scattering, which has a symmetrical angular distribution. At ultraviolet and visible wavelengths Rayleigh scattering is quite pronounced, while scattering for wavelengths greater than 3 μm is basically nonexistent. Scattering by particles comparable in size to the wavelength is called Mie scattering, whereas scattering by particles much larger than the wavelengths (i.e. water droplets) can be described using geometrical optics. Unlike Rayleigh scattering, this type of scattering is more concentrated in the forward direction.

Molecular absorption and scattering effects are often combined and can be described by a single attenuation coefficient α which can be written aș

$$\alpha(\lambda) = \alpha_A(\lambda) + \alpha_S(\lambda) \tag{2.16}$$

where α_A and α_S are the coefficient parameters describing molecular absorption and scattering processes, respectively. The transmittance τ of laser radiation that has propagated a distance *L* is related to the attenuation coefficient α as described by

$$\tau = \exp\left[-\alpha(\lambda)L\right] \tag{*2.17*}$$

where the product αL is called the optical depth. Both absorption and scattering are deterministic effects that are quite well known and can be predicted based on a variety of conditions.

2.3.2 Optical Turbulence

Other serious optical effects on a propagating laser beam are generally those caused by temperature variations manifested as refractive index fluctuations, commonly referred to as optical turbulence. In the visible and near infrared regions of spectrum, these index of refraction fluctuations are caused almost exclusively by temperature fluctuations; whereas in the far infrared region, humidity fluctuations may also contribute. Fluctuations in the index of refraction are related to corresponding temperature and pressure fluctuations. In particular, the refractive index of atmosphere *n* at a point **r** in space for optical wavelengths can be approximated according to [7]

$$n(r) \cong 1 + 79 \times 10^{-6} \frac{P(r)}{T(r)} \tag{2.18}$$

where ***P*** is the pressure in millibars and ***T*** is the temperature in Kelvin.

Optical turbulence in the atmosphere can be characterized by three parameters: outer scale L_0 , inner scale l_0 , and the structure parameter of refractive index fluctuations C^2_n, which is a measure of the strength of the optical turbulence. An effective outer scale of turbulence is defined as the largest cell size at which turbulent energy is injected into a region. Near the ground, the outer scale is assumed to grow linearly with the height above ground. An effective inner scale of turbulence is identified with the smallest cell size before energy is dissipated into heat, and is usually on the order of millimeters (near the ground). The continuous distribution of cell sizes between the inner scale and outer scale forms the inertial subrange.

The refractive index structure parameter is considered the most critical parameter along the propagation path in characterizing the effects of

atmospheric turbulence. It is usually defined as the proportionality constant in the refractive index structure function. Under statistically homogeneous and isotropic conditions, the refractive index structure function D_n in the inertial subrange exhibits the asymptotic behavior [19]

$$D_n(r) = \left\langle [n(0) - n(r)]^2 \right\rangle = C^2{}_n r^{2/3} \tag{2.19}$$

where *r* is the separation between two points in space. The classic 2 3 power law behavior was originally suggested by Kolmogorov on the basis of dimensional analysis. Values of C_n^2 for horizontal paths near the ground generally vary between 10-15 to 10-12 m-2/3, in which the latter is considered strong turbulence.

2.4 Direct Detection Model

The simplest implementation of an optical receiver is a power-detecting receiver, also called a non-coherent or direct detection receiver. Because it responds only to the instantaneous power of the collected field, a direct detection receiver does not use the transverse spatial coherence of the transmitted optical field. In a typical model of a direct detecting FSO system, the information is intensity modulated onto an optical source and transmitted through an atmospheric channel to the receiver. The receiving lens collects a portion of the received optical field and focuses it onto a photodetector.

The optical field is always photodetected in the presence of various noise sources present in the optical detection process. In FSO systems, background radiation such as natural light, is also collected along with the transmitted optical field and is usually treated as an additive noise to the desired signal field. Another source of noise is the shot noise originating in the photodetection

process and dark current at the photodetector itself. Lastly, the Johnson noise is also present in the electronic circuitry following the photodetection process. Fig. 2.3 shows the typical model for a direct detection system.

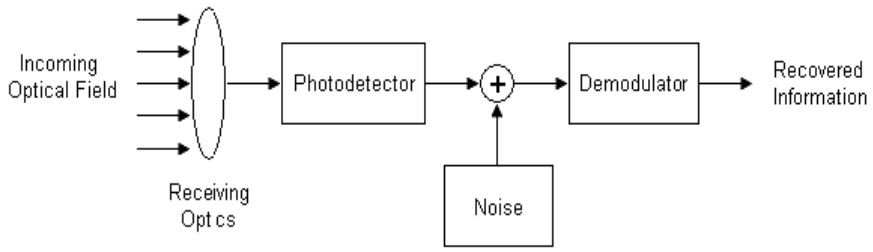

Figure 2.3: Block diagram of direct detection optic al receiver.

Recall that free space propagation of a laser beam can be modeled using a Gaussian beam with intensity profile described in Eq. (2.6). If the receiver has an aperture diameter *D* then the received signal power P_R at the photo detector is[7]

$$P_R = \int_0^{2\pi}\int_0^{\infty} I(r,L)\,r\,dr\,d\theta \cong \frac{\pi D^2}{8} I(0,L) \tag{2.20}$$

Assuming a *pin* photo detector is used, the output signal current induced by the incident optical wave is

$$i_S = \Re P_R \tag{2.21}$$

where $\Re$ is the photo detector responsivity. Let the detector be followed by a filter of bandwidth Δf , where the bandwidth is chosen to match the frequency spread of the incoming signal envelope. If all noise sources have zero mean and are statistically independent of each other, then the total noise power in the detector current $\sigma^2{}_N$ is defined by

$$\sigma^2{}_N = 2q(i_S + i_D + i_B)\Delta f + \frac{4kT\Delta f}{R} \tag{2.22}$$

where i_D and i_B are the photo detector dark current and background illumination induced currents.

2.4.1 Signal-to-Noise Ratio in Direct Detection

To quantify the performance of a direct detection receiver, the output signal-to-noise ratio (SNR) is defined as the ratio of the detector signal power to the total noise power. In practice, the received power is typically large enough such that the signal current dominates over the dark current and background illumination noise. Therefore, the remaining noise terms are typically caused by shot noise and Johnson noise[7], which gives a SNR expression for direct detection as $\Gamma_{0,DD}$

$$\Gamma_{0,DD} = \frac{i^2{}_S}{\sigma^2{}_N} = \frac{i^2{}_S}{2qi_s\Delta f + 4kT\Delta f / R} \tag{2.23}$$

If the shot noise dominates over the Johnson noise, then the resulting shot noise limited SNR $\Gamma_{0,DD-SNL}$ is given by

$$\Gamma_{0,DD-SNL} = \frac{i_S}{2q\Delta f} = \frac{\eta P_R}{2h\nu\Delta f} \tag{2.24}$$

equation 2.28 represents the quantum limit performance that can be achieved using direct detection system.

Fig. 2.4 illustrates the computed SNR performance of direct detection system for link distances of 100 m and 1 km. The transmitted laser power varies from 1 to 100 mW. The receiver uses a *pin* photodiode with responsivity of 0.45 A/W, which corresponds to approximately 70% efficiency at 785 nm wavelength. The transmitted beam has 2 mrad beam divergence and the receiver aperture has 100 mm diameter. The bandwidth of the receiver circuits is set at 1 GHz, which is quite common in FSO communication system. The shot noise limited SNR performance can be approached when the transmitted power is made high. For links beyond 1 km, the use of laser power higher than 100 mW is required to approach this ideal performance.

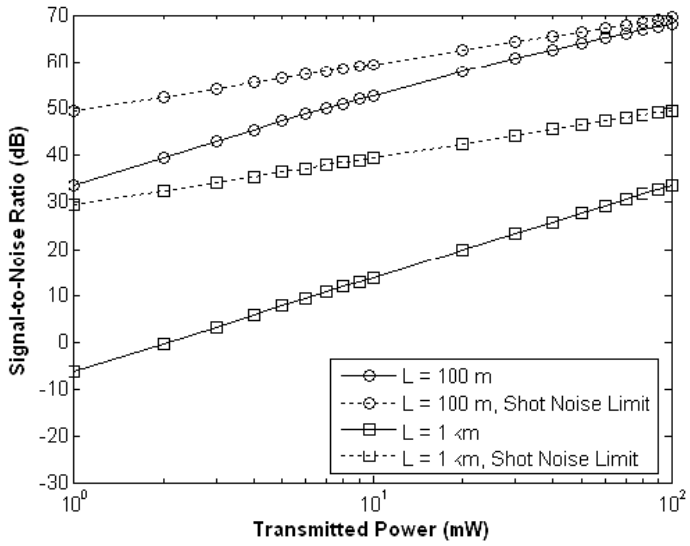

Figure 2.4: SNR performance of direct detection FSO system with θ_B =2mrad, $\Re$ =0.45 A/W, *D* =100 mm, and Δf =1 GHz; calculated for 100 m and 1 km links. [10]

2.5 Bit Error Rates in FSO links

Bit-Error-Rate (BER) depends on average received power, the scintillation over the aperture, and the receiver noise (consisting primarily of Johnson and shot noise). It also depends strongly on the decision level setting in the receiver.

The atmosphere fluctuates relatively slowly; in fact, there is not much fluctuation on time scales below about 1ms. Consequently, at high data rates, large numbers of bits are transmitted through a channel that is in a “frozen” state, but for successive groups of bits the characteristics of the channel slowly change. Consequently, the BER is constantly changing due to such fluctuations caused by atmospheric turbulence.

In the absence of turbulence, the BER can be calculated by assuming the errors result from receiver noise. This can be determined from the shot and Johnson noise originating in the receiver. In the presence of turbulence, there is an additional dominating factor that needs to be added to the noise in the BER calculations originating from the intensity fluctuations caused by turbulence. Such fluctuations are only apparent for a received “one”, since a received “zero” implies no received signal. By averaging over the appropriate intensity distribution function, and using the function describing the probability of making an error in detecting a “one”, an average BER can be calculated for different log intensity variances.

There are several techniques for detecting the signal, which ordinarily rely on a threshold device of some kind. Only when the output of the detector exceeds the set threshold value do we say a signal is present. False alarms occur when the noise alone exceeds the threshold value and is interpreted as the presence of a signal. On the other hand, if the signal plus noise does not exceed the threshold, it is called missed detection. Threshold detection concepts are illustrated in Figure 2.5 [7]

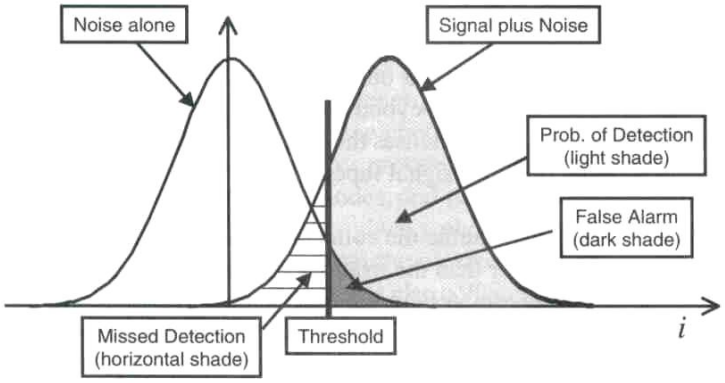

Figure: 2.5: Probability of detection and false alarm.

In on-off keyed (OOK) systems, the probability distributions of either noise alone or signal plus noise is assumed to be Gaussian. Thus, if the threshold level is set at half the average signal level *"I/2"*, then a "one" error results if the signal *I/2I* plus detector noise is less than (2$^{I/2I+i_N<I/}$ which means$^{i_N<-I/2}$). A "zero" error results if the detector noise is greater than (2). Hence, the overall probability of error is, $^{I/2i_N>I/}$

$$BER = \frac{1}{2}(p_{one} + p_{zero})$$
$$= \frac{1}{2}[P(i_N < -I/2) + P(i_N > I/2)].$$

The BER can be written as, [7]

$$BER = \frac{1}{2\sigma\sqrt{2\pi}}\left(\int_{-\infty}^{-I/2} e^{-x^2/2\sigma^2}dx + \int_{I/2}^{\infty} e^{-x^2/2\sigma^2}dx\right) \quad (2.25)$$
$$= \frac{1}{2}\left[\frac{1}{2}erfc\left(\frac{1}{2\sqrt{2}}\sqrt{\frac{S}{N}}\right) + \frac{1}{2}erfc\left(\frac{1}{2\sqrt{2}}\sqrt{\frac{S}{N}}\right)\right]$$
$$= \frac{1}{2}erfc\left(\frac{1}{2\sqrt{2}}\sqrt{\frac{S}{N}}\right).$$

Chapter 3

Modulation Schemes in Optical Wireless Communications

3.1 Intensity Modulated Direct Detection (IM/DD) systems

For optical wireless communication systems, most frequently used system is Intensity Modulated Direct Detection *(IM/DD)* system. In optical wireless systems, the intensity of an optical source is modulated to transmit signals. For digital data transmission, there is no practical alternative to digital modulation since it provides source coding (data compression), channel coding (error detection/correction), and easy multiplexing of multiple information streams [21]. The transmission of the digital data can be done on a bit-by-bit basis (binary encoding) or on a bit-word basis (block encoding). Several baseband modulation schemes for binary and block encoding are discussed; and their performance in terms of power and bandwidth efficiency is compared.

3.1.1 On-Off Keying

The simplest type of binary modulation scheme is OOK. In an active high OOK encoding, a ‘one’ is coded as a pulse, while a ‘zero’ is coded as no pulse or off field. To restrict the complexity of the modulator, the pulse shape is chosen to be rectangular. The bit rate is denoted as $R_B = 1/T_b$, where T_b is the bit duration; and is directly related to the rate at which the source can be switched on and off. The normalized transmit pulse shape for OOK is given by [11]

$$p(t) = \begin{cases} 1 & \text{, for } t \in [0, T_b) \\ 0 & \text{, elsewhere} \end{cases}. \qquad (3.1)$$

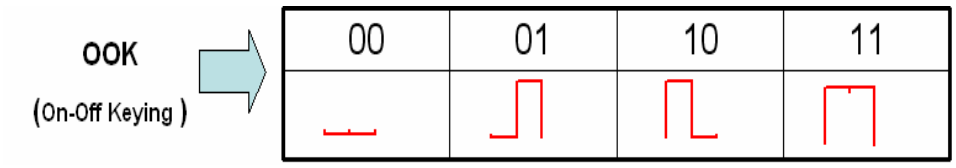

In the demodulator, the received pulse is integrated over one bit period, then sampled and compared to a threshold to decide a 'one' or 'zero' bit. This is called the maximum likelihood receiver, which minimizes the bit error rate (BER). Because of detector noise, errors may be made in determining the actual symbols transmitted. In OOK transmission, the random noise can be approximated as Gaussian distribution. Assuming both symbol have identical noise variance and are equally likely to be transmitted, the threshold level is set halfway between the symbols currents. Thus, the BER can be calculated as in [21, 26]

$$\Pr(e)_{OOK} = \frac{1}{2} erfc\left(\frac{i_s}{2\sqrt{2}\sigma_N}\right) = \frac{1}{2} erfc\left(\frac{1}{2\sqrt{2}}\sqrt{\Gamma_0}\right) \tag{3.2}$$

Where $erfc(x) = (2\pi)^{-1/2}\int_0^{\infty} \exp(-t^2)dt$ and Γ_0 is the SNR for direct detection Receiver defined in Eq. (2.23).

3.1.2 Pulse Position Modulation

In block encoding, bits are transmitted in blocks instead of one at a time. Optical block encoding is achieved by converting each word of *l* bits into one of $L = 2^l$ optical fields for transmission. One of the most commonly used optical block encoding schemes is PPM, where an input word is converted into the position of a rectangular pulse within a frame. The frame with duration T_f is divided into *L* slots and only one of these slots contains a pulse. This scheme can also be denoted as *L* PPM, in order to emphasize the choice of *L*. The transmit pulse shape for *L*-PPM is given by [11]

$$p_m(t) = \begin{cases} 1 & , \text{ for } t \in \left[(m-1)T_f/L, mT_f/L\right) \\ 0 & , \text{ elsewhere} \end{cases}$$

(3.3)

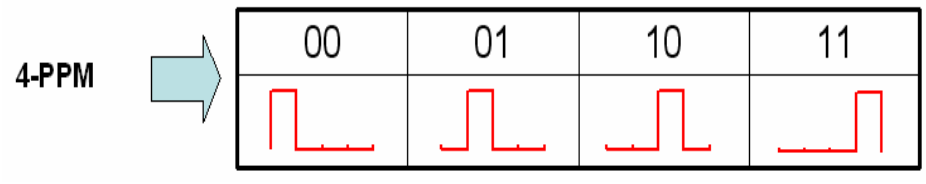

Where $m \in \{1,2,....,L\}$ Since L possible pulse positions code for $\log_2 L$ bits of information, the bit rate is $R_b = \log_2 L/T_f$

The optimum L-PPM receiver consists of a filter bank, each integrating the photocurrent in one pulse interval. The demodulated pulse is taken to originate from the slot in which the most current level was found. If the demodulated pulse position is the correct pulse position, $\log_2 L$ bits are decoded correctly. Otherwise, we assume that all L -1 wrong position are equally likely to occur. Therefore bit errors usually occur in groups. For Gaussian noise, the BER can be written as [20, 21]

$$\Pr(e)_{PPM} \approx \frac{1}{2} erfc\left(\frac{1}{2\sqrt{2}}\sqrt{\frac{L}{2}\log_2 L\Gamma_0}\right) \qquad (3.4)$$

Substituting L = 2 yields the BER for Manchester signals, which is identical to the BER of OOK modulation.

3.2 Comparison of Modulation Schemes

In order to compare different modulation schemes, the power and bandwidth efficiency, defined as the required power and bandwidth at a desired transmission speed and BER quality, were calculated.

3.2.1 Power Efficiency

Power efficiency can readily be derived from the BER expressions. Fig. 3.1 shows the BER performance of OOK, for both NRZ and RZ, and *L*-PPM for *L* =2, 4, and 8. It is fairly obvious that 8-PPM has the best BER performance, and hence is the most power efficient scheme. To achieve a given BER value p_e, the power requirement in OOK and *L*-PPM scheme can be written as [11]

$$P_{OOK} = 2\sqrt{2}\,\frac{\sigma_N}{\Re}\,erfc^{-1}(2p_e)$$

and

$$P_{PPM} = 2\sqrt{2}\,\frac{\sigma_N}{\Re}\left(\frac{L}{2}\log_2 L\right)^{-1/2} erfc^{-1}(2p_e) = \frac{P_{OOK}}{\sqrt{\frac{L}{2}\log_2 L}}$$

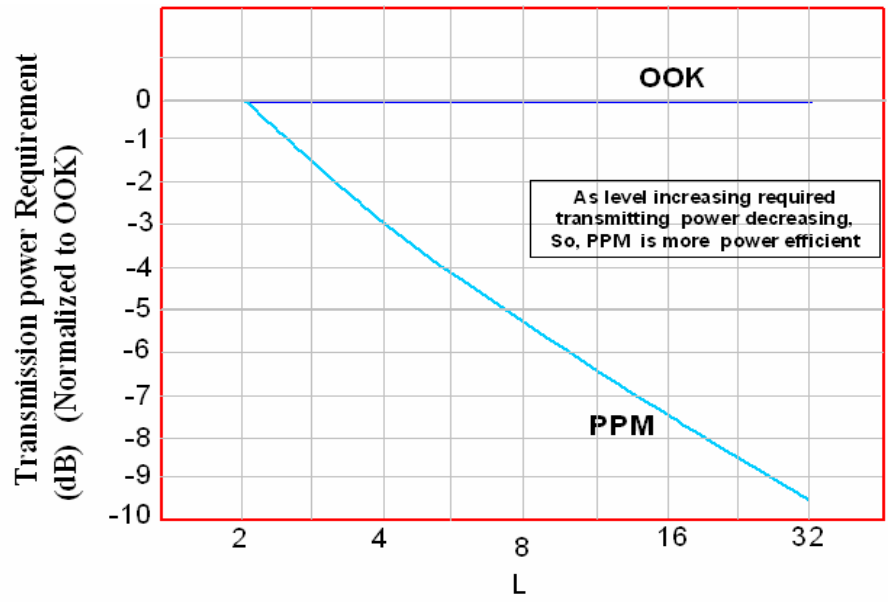

Figure 3.1: Transmission power comparisons of PPM and OOK

Thus, it is evident that *L*-PPM requires a factor of $\sqrt{(L/2)\log_2 L}$ less power than OOK to obtain a particular BER performance.

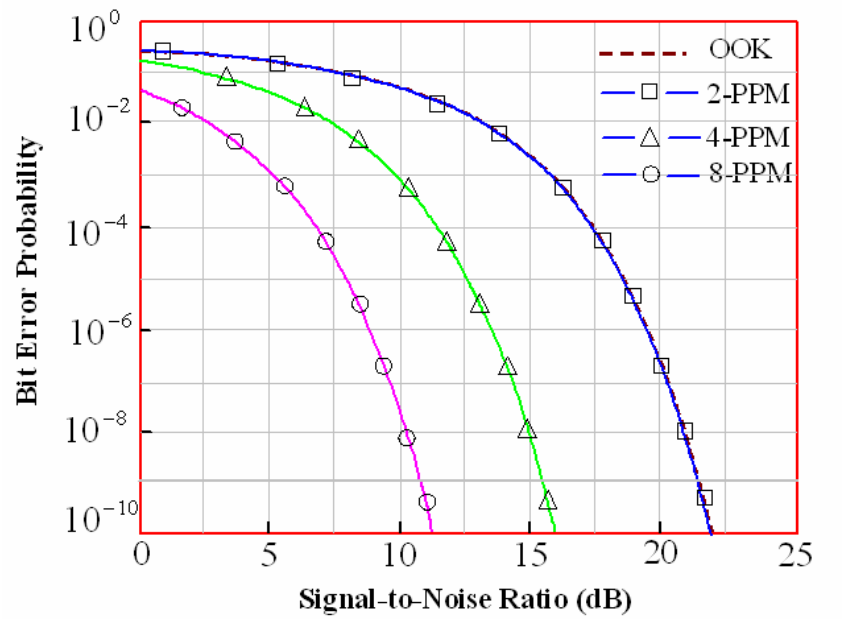

Figure 3.2: BER performance for OOK from Eq. (3.3), and *L*-PPM (*L* =2 , 4, and 8), from Eq. (3.4).

3.2.2: Bandwidth Efficiency

Another important measure of performance is the bandwidth efficiency. The bandwidth required for modulation can be estimated from the first zero of the transmitted signals power spectrum. Fig. 2.9 illustrates the spectral density envelope (without the Dirac impulses) of the transmitted signals for OOK and *L*-PPM. Note that only positive frequency is shown and the frequency is normalized to the bit rate R_b. The bandwidth efficiency is defined as the ratio between bit rate and required bandwidth (in bps/Hz). The required bandwidth is $B_{req} = R_b$ for OOK and $B_{req} = LR_b / \log_2 L$ for *L*-PPM.[11]

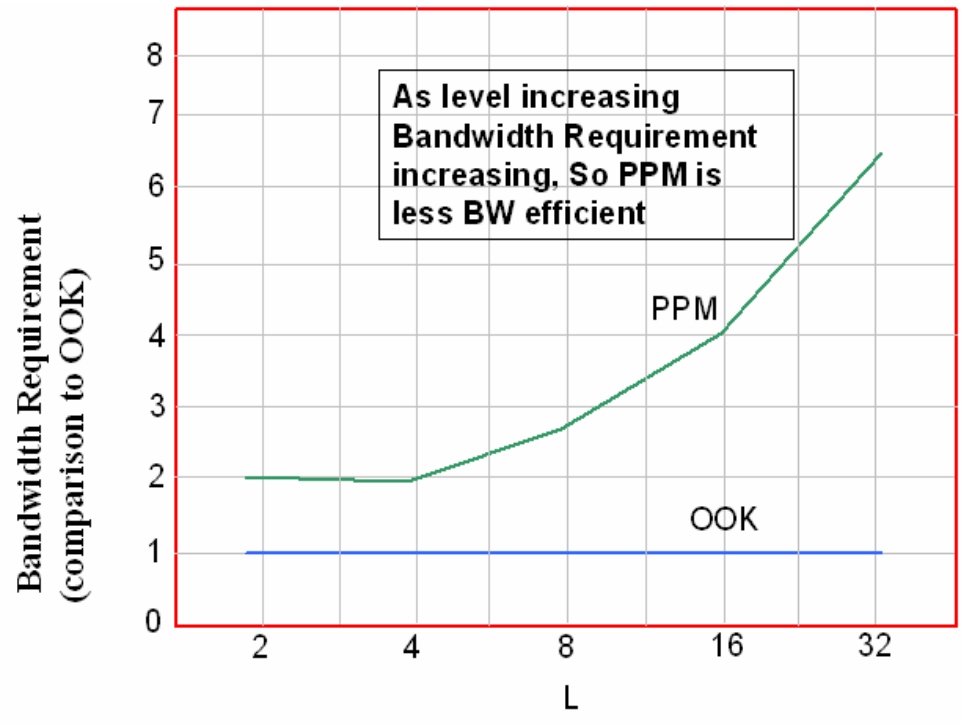

Figure 3.3: Bandwidth requirement compared to OOK.

Thus, the bandwidth efficiency of *L*-PPM can be shown to be at least 1.9 times worse than OOK. To conclude, the comparison results are also summarized in

Table 3.1: Comparison of baseband intensity modulation techniques[11].

	Bandwidth Requirement	Power Requirement
OOK	R_b	P
L-PPM	$R_b(L/\log_2 L)$	$P/\sqrt{\{(L/2)(\log_2 L)\}}$

3.2.3 Effects of Timing Error on Performance

All the modulation schemes previously discussed require accurate pulse or slot integrations for ideal decoding. These integrations must be clocked by

auxiliary timing circuits that provide the start and stop markers for the integrators, so that the integration variables are produced only over the exact slot times. If the timing is not accurate, the integrations occur over offset intervals, leading to false integration values that can degrade the decoding performance. In OOK system, the timing errors essentially cause additional variations in signal current, which can be viewed as additional noise source, hence always degrade the performance. Thus, they must be maintained to a small fraction of the bit time for adequate decoding.[12]

In a PPM based system, the decoding process does not perform a threshold test, but rather an integrator comparison test. Timing offsets cause loss in pulse energy in the correct interval, and consequently a build-up of energy in the incorrect interval. This causes relatively faster decrease in performance as the offset is increased relative to the pulse time. For Manchester signals, since the slot interval is only half the bit interval, they are more susceptible to timing errors than the OOK system. Furthermore, the slot timing capability places a lower limit on the slot times that can be used in PPM systems, limiting their advantage over OOK systems.

Chapter 4

The Effects of Atmospheric Turbulence on Link Performance

4.1 Turbulence Overview

Unfortunately, the atmosphere is not an ideal communication channel. Atmospheric turbulence can cause fluctuations in the received signal level, which increase the bit errors in a digital communication link. In order to quantify the performance limitations, a better understanding of the effect of the intensity fluctuations on the received signal at all turbulence levels is needed.

The local density of the atmosphere is constantly fluctuating because of temperature and pressure fluctuations. This is atmospheric turbulence.

When a laser beam propagates through the atmosphere the randomly varying spatial distribution of refractive index that it encounters causes a number of effects. These include:

(1) A fluctuating intensity as observed with an optical detector at the end of the path. This is referred to as scintillation.

(2) A varying degree of fluctuation with the size of the detector, or with the size of the receiving optics that direct the collected light to the detector. This is called aperture averaging.

(3) If a circularly symmetric Gaussian beam is observed at different distances from a transmitter it suffers progressive deterioration with increasing distance and turbulence strength. The progressive changes that are observed are:

(i) Deviations of the beam shape from circular that are time dependent;

(ii) Wander of the centroid of the beam;

(iii) Increase in the width of the beam over and above that expected from diffraction.and

(iV) Breakup of the beam into distinct patches of illumination whose shapes and locations fluctuate with time.

(4) The “coherence length” of the laser beam falls.

(5) The angle of arrival of the phase fronts at a receiver fluctuates.

Winds, which move the atmosphere in a more correlated way, can cause the centroid of the beam to shift, but they do not intrinsically randomize the laser beam as does turbulence. In principle, the effects of correlated atmospheric effects that “steer” a laser beam can be compensated with a beam-steering scheme at the transmitter. [7]

4.2 Optical Wave Propagation in Atmospheric Turbulence

Theoretical studies of optical wave propagation are traditionally classified as belonging to either weak or strong fluctuations theories. For weak intensity fluctuations, the most widely used analysis method is the classical Rytov approximation [22]. Its most useful results for free space optical (FSO) performance analysis is the expressions for the mean and covariance functions of received intensity fluctuations. The presence of optical turbulence will always degrade the performance of FSO system because of the randomness of the received signal. To evaluate this performance mathematically, distribution models for intensity fluctuations are required.

4.2.1 Mean of Intensity Fluctuations

The MCF of the optical field determines, among other quantities, the mean intensity of the field can be written as [7]

$$m_2(r_1, r_2, L) = M_2(r_1, r_2, L)\exp\left[\sigma^2{}_r(r_1, L) + \sigma^2{}_r(r_2, L) - T\right] \times \exp\left[-\frac{1}{2}\Delta(r_1, r_2, L)\right] \tag{4.1}$$

where $\sigma_r^{\,2}(r, L) = [E_2(r, r) - E_2(0,0)]/2$ describes the atmospherically induced change in the mean intensity profile in the transverse direction, and $T = -2E_1(0,0) - E_2(0,0)$ describes the change in the on-axis mean intensity at the receiver plane caused by turbulence. The last exponential term is the complex degree of coherence, where [7]

$$\Delta(r_1, r_2, L) = E_2(r_1, r_1) + E_2(r_2, r_2) - 2E_2(r_1, r_2) \tag{4.2}$$

Evaluating this MCF at $r_1 = r_2 = r$ leads to an expression for the mean $\langle I \rangle$ intensity fluctuations

$$\langle I(r, L)\rangle = I_0 \frac{w_0}{w^2{}_L}\exp(-\frac{2r^2}{w^2{}_L})\exp[2\sigma^2{}_r(r, L) - T] \tag{4.3}$$

from which the additional beam spread due to turbulence can be deduced. The expressions for $\sigma^2{}_r$ and *T* evaluated using the Kolmogorov spectrums are given by [7]

$$\sigma^2{}_r(r,L) = 1.11\sigma^2{}_R A^{5/6} \frac{r^2}{w^2{}_L} \tag{4.4}$$

$$T = 1.33\sigma_R{}^2 A^{5/6} \tag{4.5}$$

where $\sigma_R{}^2$ is the Rytov variance. From these two results, the mean intensity profile can be approximated by the Gaussian function [23]

$$\langle I(r,L)\rangle \cong I_0 \frac{w^2{}_0}{w^2{}_E} \exp(-\frac{2r^2}{w^2{}_E}) \tag{4.6}$$

where w_E is a measure of the effective beam spot size affected by turbulence defined as

$$w_E = w_L[1+1.33\sigma^2{}_R A^{5/6}]^{1/2} \tag{4.7}$$

This expression is considered a measure of the turbulence induced beam spreading, which increases the beam width beyond normal diffraction effects.

4.2.2 Covariance Function of Intensity

If the collecting receiver aperture is larger than the coherence length, the fluctuations will be spatially averaged, hence reducing the intensity variance by a factor of *A* [16, 23]

$$A = \frac{\sigma^2{}_I(D)}{\sigma^2{}_I} \approx \left[1+1.06(\frac{kD^2}{4L})\right]^{-7/6} \tag{4.8}$$

where $\sigma^2{}_I(D)$ is the intensity variance averaged over an aperture with diameter *D*.

The effects of aperture averaging in reducing the scintillation index on FSO links have also been observed experimentally [24, 25]. Fig. 4.1 shows the aperture averaging factor as a function of receiver aperture diameter for a 1 km link. It shows that using an aperture diameter of 200 mm can reduce the intensity variance by a factor of $5.55\ 10^{3}$. Although the Rytov variance suggests that scintillation index can increase without limit, this is never experimentally observed since the scintillation is saturated and is typically limited to the order of unity. For a receiver with 200 mm aperture diameter, the averaging effect can reduce the intensity variance to the weak fluctuation regime.

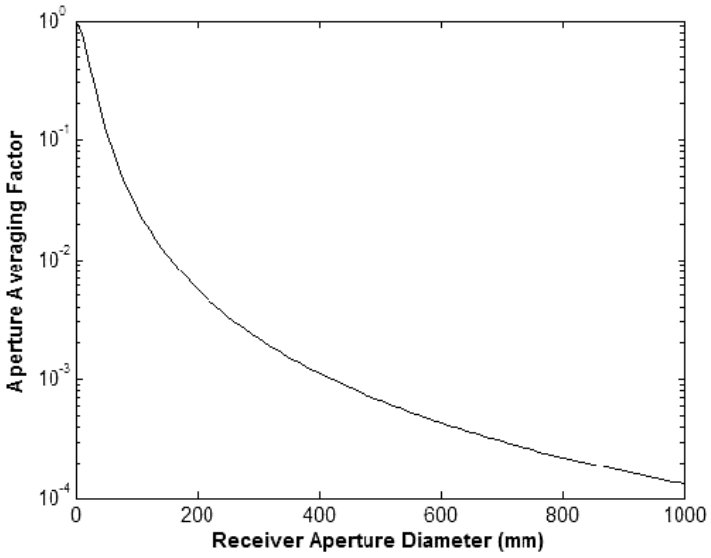

Figure 4.1: Aperture averaging factor versus receiver aperture size calculated from Eq. (4.8) for L =1 km and λ =785 nm.[7]

4.2.3 Distribution Models for Intensity Fluctuations

The performance of an FSO system with an atmospheric turbulence channel can be evaluated mathematically with knowledge of the probability

density function (PDF) of the randomly fading intensity signal. The PDF for the intensity fluctuations p_I is the lognormal distribution [7]

$$p_I(i) = \frac{1}{i\sqrt{2\pi\sigma^2{}_I}} \exp\left\{ -\frac{1}{2\sigma^2{}_I}\left[\ln\left(\frac{i}{\langle I(r,L)\rangle} \right) + \frac{1}{2}\sigma^2{}_I \right]^2 \right\}, i > 0 \qquad (4.9)$$

where the intensity variance $\sigma^2{}_I$ can be obtained from the Rytov variance $\sigma^2{}_R$

4.3 SNR and BER for Atmospheric Turbulence

The most practical implementation for FSO communication involves the use of an intensity modulation/direct detection (IM/DD) system. The transmitted data is on-off keying (OOK) intensity modulated and goes through an atmospheric channel to the receiver. The receiver aperture collects the received optical signal and focuses it onto a photo detector, which converts the instantaneous optical power into electrical current for the detection process. In the presence of atmospheric turbulence between transmitter and receiver, the received signal exhibits random intensity fluctuations. Thus, the instantaneous received signal power P_R as expressed in Eq. (2.20) is a random quantity. The observed quantity is now the averaged or mean received signal power P_R given by

$$\langle P_R \rangle \cong \frac{\pi}{8} D^2 \langle I(0,L) \rangle = \frac{P_R}{1 + 1.33\sigma_I{}^2 A^{5/6}} \qquad (4.10)$$

Furthermore, it follows that the mean signal current is $\langle i_S \rangle = \Re \langle P_R \rangle$ where $\Re$ is the photo detector responsivity. The output current from the detector $i = i_S + i_N$ in this case is a random variable, which has the mean value $\langle i_S \rangle$ and the variance

$\sigma_i^{\,2} = \sigma_S^{\,2} + \sigma_N^{\,2}$ where $\sigma_S^{\,2}$ represents fluctuations in the signal that become a contributor to the detector noise and related to the normalized intensity variance $\sigma_I^{\,2}$

$$\sigma_S^{\,2} = \left\langle i_S^{\,2} \right\rangle - \left\langle i_S \right\rangle^2 = \left\langle i_S \right\rangle^2 \sigma_I^{\,2} \tag{4.11}$$

using the relations given in Eqs. (4.10) and (4.11), and the definition of the output signal-to-noise ratio (SNR) in the absence of optical turbulence Γ_0 given in Eq. (2.23), the averaged SNR $\langle \Gamma_0 \rangle$ at the output of the detector assumes the form

$$\langle \Gamma_0 \rangle = \frac{\left\langle i_S \right\rangle^2}{\sigma_i^{\,2}} = \frac{\Gamma_0}{(1 + 1.33\sigma_I^{\,2} A^{5/6})^2 + \Gamma_0 \sigma_I^{\,2}} \tag{4.12}$$

Thus, the presence of turbulence induced signal fluctuations will always deteriorate the SNR performance of IM/DD FSO system. Fig. 4.2 illustrates the mean SNR performance for three different normalized intensity variance values.

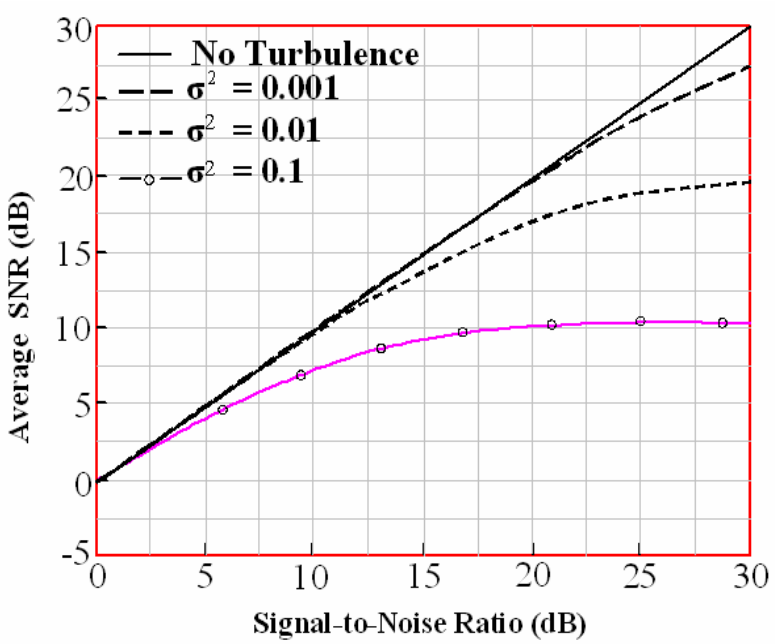

Figure 4.2: Average SNR performance in the presence of optical turbulence with σ^2 =0.001, 0.01, and 0.1; calculated from Eq. (4.12) for ***A***=0.001.

In the presence of optical turbulence, the bit error rate (BER) expression must be modified to incorporate the effects of signal fluctuations. In this case, the threshold level is now set to half the average signal corresponding to a received pulse $\left(i_T = \langle i_S \rangle / 2\right)$ The false alarm probability P_f does not depend on the random received signal and can be written as[9]

$$P_f = \Pr(1|0)\frac{1}{2}erfc\left(\frac{1}{2\sqrt{2}}\sqrt{\langle \Gamma_0 \rangle}\right) \tag{4.13}$$

However, the miss probability P_m is now

$$P_m = \Pr(0|1)\frac{1}{2}erfc\left(\left[\frac{2i_S}{\langle i_S \rangle} - 1\right]\frac{1}{2\sqrt{2}}\sqrt{\langle \Gamma_0 \rangle}\right) \tag{4.14}$$

where i_S is the random detector signal corresponding to the instantaneous received intensity. To compute the average BER $\langle \Pr(e) \rangle$ these equations must be averaged over the intensity fluctuation spectrum. This gives

$$\langle \Pr(e) \rangle = \frac{1}{4}\left\{ erfc\left(\frac{1}{2\sqrt{2}} \sqrt{\langle \Gamma_0 \rangle} \right) + \int_0^\infty p_I(i_S)\, erfc\left(\left[\frac{2i_S}{\langle i_S \rangle} - 1 \right] \frac{1}{2\sqrt{2}} \sqrt{\langle \Gamma_0 \rangle} \right) di_S \right\} \qquad (4.15)$$

where $P_I(i)$ is the PDF of the intensity fluctuations.

The limiting performance of the average BER can be achieved by assuming the threshold level is dynamically set at half the instantaneous received signal level $i_T = i_s / 2$ which leads to the expression

$$\langle \Pr(e) \rangle_L = \frac{1}{2} \int_0^\infty p_I(i_s)\, erfc\left(\frac{i_s}{2\sqrt{2}\langle i_s \rangle} \sqrt{\langle \Gamma_0 \rangle} \right) di_s \qquad (4.16)$$

Fig. 4.3 shows the numerical computation of theoretical BER for a FSO system as a function of no turbulence SNR using both Eqs. (4.15) and (4.16). While the expression in Eq. (4.15) gives a more accurate description of practical systems, the expression in Eq. (4.16) is more elegant and mathematically convenient. Observe that for different intensity variances in the weak fluctuation regime, the performance of the practical system approaches ideal system performance limit. We will use Eq. (4.16) when deriving an expression for the theoretical performance limit, and Eq. (4.15) when a more accurate model is needed for comparison with experimental results.

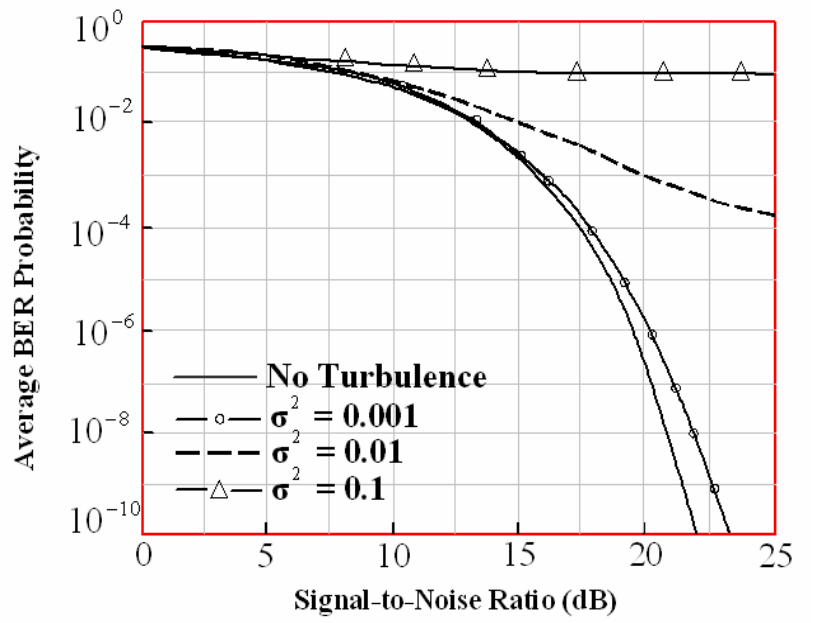

Figure 4.3: Theoretical BER performance of FSO system using constant threshold, From Eq. (4.15), and dynamic threshold, from Eq. (4.12); calculated for σ^2=0.001, 0.01, and 0.1. The solid curve depicts BER performance in the absence of turbulence.

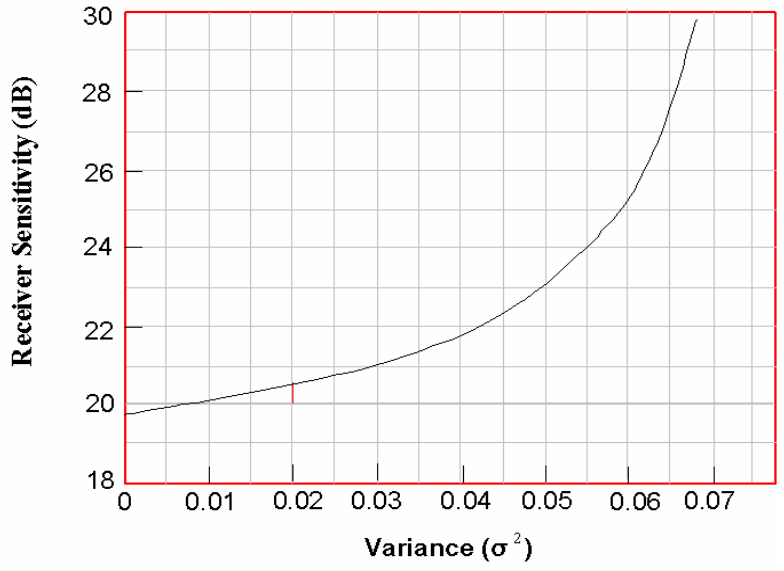

Figure 4.4: Receiver Sensitivity Vs Variance

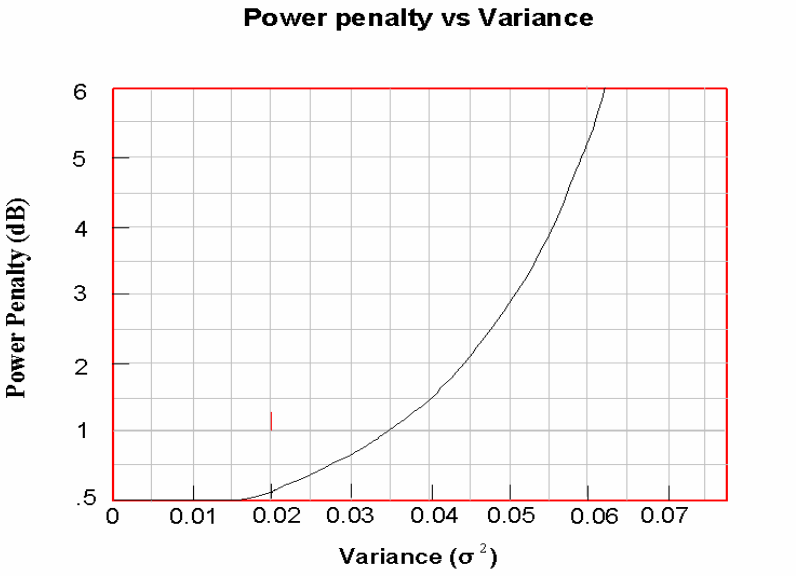

Figure 4.5: Power Penalty Vs Variance

Chapter 5

Conclusions and Future Works

5.1 Conclusions

In this thesis the characteristics and properties of several important design parameters in FSO communication systems are discussed using the curve analysis and proposed the simple and flexible modulation techniques for the outdoor use in FSO system and the performance degradation by the atmospheric turbulences.

Here we found a semiconductor laser or laser diode is the preferable type of optical source used in transmitter systems because of its fast modulation capability, narrow linewidth, moderately high power, and small production cost. For single mode laser diodes, the beam propagation in free space can be correctly modeled as a Gaussian beam. This model predicts the divergence of the beam as it propagates away from the source, decreasing the received optical power by a receiver system. This free space loss in FSO system may be compensated by beam forming optics, which provides directivity and gain similar to antennas in RF system.

At the receiver system, photodiodes are used almost exclusively in the photodetection process because they have high sensitivity and fast response time. For FSO communications, when the transmission rate is below one gigabit per second, the use of *pin* photodiodes in combination with electronic post-amplifiers is preferable to the use of APDs. The presence of noise limits the ability of a receiver to detect an incoming signal, which is typically characterized by the SNR. The two most important noise sources typically used in assessing the SNR of FSO systems are the shot noise and the thermal noise. The SNR is also affected by the degradation of the optical signal traveling through the atmospheric channel. In addition to free space loss, the atmosphere also introduces attenuation caused by either molecular absorption or scattering, and fading caused by optical turbulence.

For optical wireless communication systems, most frequently used system is Intensity Modulated Direct Detection *(IM/DD)* system. In optical wireless systems, the intensity of an optical source is modulated to transmit signals. . For FSO systems, although the power efficiency is inferior to PPM, OOK encoding is more commonly used due to its efficient bandwidth usage and robustness to timing errors. Therefore, in this research work, For FSO systems we prefer intensity modulation/direct detection (IM/DD) with an OOK technique.

Unfortunately, the atmosphere is not an ideal communication channel. Atmospheric turbulence can cause fluctuations in the received signal level, which increase the bit errors in a digital communication link. In order to quantify the performance limitations, a better understanding of the effect of the intensity fluctuations on the received signal at all turbulence levels is needed. In the presence of atmospheric turbulence between transmitter and receiver, the received signal exhibits random intensity fluctuations. Thus, the instantaneous received signal power will be averaged and thus the mean SNR will be introduced. The bit error rate (BER) expression must be modified to incorporate the effects of signal fluctuations. The limiting performance of the average BER can be achieved by assuming the threshold level is dynamically set at half the instantaneous received signal level .From the bit error probability (BER) vs. SNR (figure: 4.3) and the power penalty curve (figure: 4.5) we found that how much the signal degrades and the power loss for the effect s of the atmospheric turbulences.

5.2 Future works:

The future study will be with modulation performance comparison and analysis some advanced technique to mitigate the effects of atmospheric turbulence on free space optical communication link like:

Aperture averaging of received scintillation will be studied in order to design receivers which include efficient computational techniques for Fante's correlation functions that are important in assessing the effects of turbulence in weak and strong conditions that can mitigate the negative effects of turbulence and hence optimize performance.

Future study will be the analysis of the modulation performances of some additional modulation techniques like Digital Pulse Interval Modulation *(DPIM)* turbo coded modulation and the polarization shift keying (PolSK) modulation with in FSO communications under turbulence condition

Another possible receiver improvement might be in the data recovery process. In the current system, logical addition, which assumes that the turbulence always causes a fading channel, is used. However, in reality, intensity fluctuations can cause either a fading or surging channel.

The diversity technique especially the Time delayed diversity technique**,** which takes advantage of the fact that the atmospheric path from transmitter to receiver is statistically independent for time intervals beyond the coherence time of the intensity fluctuations and Communications performance will be improved because the joint probability of error is less than the probability of error from individual channels

For networking applications, broadcasting capability is frequently required to establish and maintain communications among multiple nodes. An Omni directional FSO system, which is based on non-directed line-of-sight (LOS) technique, will evaluate to provide this important inter-node communication capability and how it can be implemented in WDM communication system.

LIST OF REFERENCES

[01] A.C. Boucouvalas, *"Challenges in Optical Wireless Communications"*, in Optics & Photonics News, Vol. 16, No. 5, 36-39 (2005).

[02] I.I. Smolyaninov, L. Wasiczko, K. Cho, C.C. Davis, *"Long Distance 1.2 Gb/s Optical Wireless Communication Link at 1550 nm"*, in *Free-Space Laser.*

[03] C.C. Davis, I.I. Smolyaninov, *"Effect of atmospheric turbulence on bit-error rate in an on-off-keyed optical wireless system,"* in *Free-Space Laser.*

[04] A. Acampora, *"Last Mile by Laser"* (Scientific American, 2002).

[05] P. Gupta, P.R. Kumar, *"The Capacity of Wireless Networks"*, IEEE Trans. Inf.Thry. **46**, 388-404 (2000).

[06] R.K. Crane, *"Electromagnetic Wave Propagation through Rain"*, (Wiley, New York, 1996).

[07] Heba Yuksel,*"Studies of the Effects of Atmospheric Turbulence on Free Space Optical Communications"*, (Ph.D. Dissertation, Univ. of Maryland, College Park, 2005).

[08] Street man *"Semiconductor Materials", book*.

[09] Djafar K Mynbaev and LoweLL. Scheiner *"Fiber-optics Communication Technology".*

[10] Linda Marie Wasiczko *"Techniques to mitigate the effects of atmospheric turbulence on free space optical Communication links"*, (Ph.D. Dissertation, Univ. of Maryland, College Park, 2004).

[11] Jinlong Zhang *"Modulation Analysis for Outdoors Applications Of Optical Wireless Communications"* 0-7803-6394-9/00/c10.00O2000 IEEE.

[12] *www.shu.ac.uk./ocr/*

[13] H. Ghafouri-Shiraz, B.S.K. Lo, *"Distributed Feedback Laser Diodes: Principles and Physical Modeling"*, (Wiley, New York, 1995).

[14] G.M. Smith, J.S. Hughes, R.M. Lammert, M.L. Osowski, G.C. Papen, J.T. Verdeyen, J.J. Coleman, *"Very narrow linewidth asymmetric cladding InGaAs-GaAs ridge waveguide distributed Bragg reflector lasers"*, IEEE Photon. Tech. Lett. **8**, 476-478 (1996).

[15] L.C. Andrews, R.L. Phillips, C.Y. Hopen, *"Aperture averaging of optical scintillations: power fluctuations and the temporal spectrum"*, Waves random Media **10**, 53-70 (2000).

[16] C.C. Davis, *"Lasers and Electro-Optics: Fundamentals and Engineering"*, (Cambridge University Press, Cambridge, 1996).

[17] G. Keiser, *"Optical Fiber Communications"*, (McGraw-Hill, 2000).

[18] R. Otte, *"Low Power Wireless Optical Transmission"*, (Delft University Press, The Netherlands, 1998). 145.

[19] A.N. Kolmogorov, *"The local structure of turbulence in an incompressible viscous fluid for very large Reynolds numbers"*, C.R. (Dokl.) Acad. Sci. USSR **30**, 301-305 (1941).

[21] E.A. Lee, D.G. Messerschmitt, *"Digital Communication"*, (Kluwer Academic Publishers, Boston, 1994).

[26] A.B. Carlson, *"Communication Systems: An Introduction to Signals and Noise in Electrical Communication"*, (McGraw-Hill, New York, 1986).

[20] J.R. Barry, *"Wireless Infrared Communications"*, (Kluwer Academic Publishers,1994).

[22] V.I. Tatarskii, *"Wave Propagation in a Turbulent Medium, trans". by R.A. Silverman*, (McGraw-Hill, New York, 1961).

[23] L.C. Andrews, R.L. Phillips, *"Laser Beam Propagation through Random Media"*, (SPIE Optical Engineering Press, Bellingham, 1998).

[24] L.M. Wasiczko, *"Techniques to Mitigate the Effects of Atmospheric Turbulence on Free Space Optical Communication Links"*, (Ph.D. Dissertation, Univ. of Maryland, College Park, 2004).

[25] H. Yuksel, *"Studies of the Effects of Atmospheric Turbulence on Free Space Optical Communications"*, (Ph.D. Dissertation, Univ. of Maryland, College Park, 2005).